# Supplementary Material

## A Computational View On the Significance of E-Ring in Binding of (+)-Arisugacin A to Acetylcholinesterase.

Ziyad F. Al-Rashid[a,*] and Richard P. Hsung[b,*]

[a]*Alchemical Research, LLC, 260 East Wall Street, Bethlehem, Pennsylvania 18018, USA.*

[b]*Division of Pharmaceutical Sciences and Department of Chemistry, University of Wisconsin, Madison, Wisconsin 53705, USA.*

**Computational Docking Studies of Acetylcholinesterase Inhibitors**

*In silico* modeling of acetylcholinesterase and small molecule docking events was performed. This study was powered by AutoDock v4.2 and the more recent AutoDock Vina,[1] made available by The Scripps Research Institute under a General Public License. X-ray crystal data and docking predictions were examined using PyMol[2] and Python Molecule View[3].

**Model Development:** X-ray crystal data[4] of (+)-territrem B- bound-*h*AChE [TB–*h*AChE] and donepizil- bound-*tc*AChE (*Torpedo Californica* AChE) were obtained from the Protein Data Bank (www.pdb.org). As noted, the reported TB–*h*AChE[4b] bound structure appears to better accommodate arisugacin-like structures with a large degree of reorganization around catalytic active site and the protein backbone in the peripheral site that led to an altered gorge shape.[4b] While *AutoDock* modeling can allow for flexibility in selected protein residues, these degrees of freedom do not account for the conformation changes seen between the donepizil-*tc*AChE (protein structure source in our 2011 study[5]) and the TB–*h*AChE[4b] active site gorge conformations. To examine these differences docking studies were performed comparing the TB–*h*AChE and the donepezil-*tc*AChE complex as sources of the protein structure for further modeling. The ligands (TB and donepezil respectively) were removed from the file, as well as all water molecules. An algorithm was utilized to add all hydrogens to the protein, with special care given to the site of protonation of histidine residues.[6] This protein structure was used as the base structure onto which small molecules would be docked. During molecular docking computations residues were either designated as flexible or rigid, the majority being rigid due to computation limitations. When residue flexibility was permitted, it was allowed in residues PHE330, TRP279, and ASP72 (*tc*AChE residue numbering, TYR337, TRP286, and ASP74 residues in *h*AChE respectively) holding the remainder of the enzyme rigid. *AutoDock* modeling can allow for flexibility in the small molecules/ligands in the form of assigned rotatable bonds. Note that throughout this study, the small molecules/ligands starting geometries were matched as closely as possible to the geometry of protein bound TB or donepizil X-ray crystal structure data. The site of molecular probing was focused to a grid box located in the active site of AChE, with the length of each side being 40 to 60 Å [**Figure 1**].

In this study, we generally observed that conformational restriction of protein residues and/or ligand rotatable bonds is accompanied by higher affinity predictions. Examination of the predicted docking events revealed that small conformational changes led to large changes in affinity predictions. Generally, conformations oriented and locked to match those observed in the X-ray crystal structure had the higher affinity predictions. When making comparison across the arisugacin and territrem families of natural products, analogs, and conformations thereof we were very careful to note, align, and restrict conformations of the docked ligand and the protein residues.

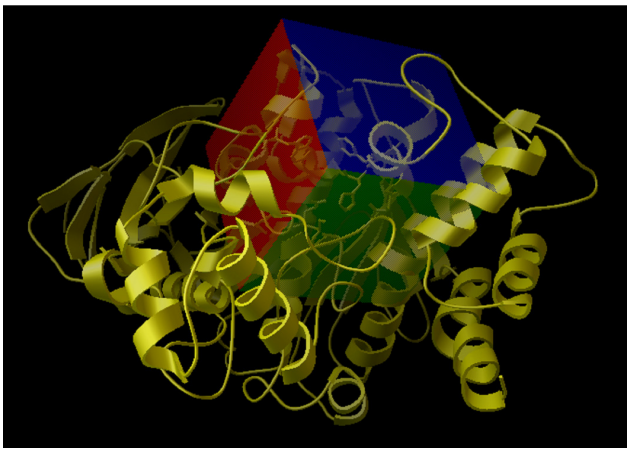

**Figure 1.** Grid box with 60 Å sides located at the active of *tc*AchE. Key residues displayed as sticks.

Herein were report on this variability of binding affinities with what is seemingly very small conformational differences. We do not offer an explanation as this is beyond the scope of our study, rather we do so to provide caution and share our findings. Some of the conformational differences are very subtle, particularly those involving the methoxy groups or the biaryl bond, however, energetically we observe ~1-2 kcal $mol^{-1}$ binding affinity differences. Such variability layered into a series of analogs would make it very difficult to discern trends. It is important to be aware of this possibility. When working in the blind, as we did in 2011, you have little choice but to allow for as much flexibility as possibly/or is feasible, or at least to gradually allow for greater flexibility and to make comparisons along the way. In general, consistency across a series of analogs is necessary, with careful attention to the positioning of rotatable bonds when making comparisons. Qualitatively this modeling package (AutoDock) has been excellent.

**Comparing TB–*h*AChE and donepezil-*tc*AchE complexes as sources of the protein structure for further modeling.**

In addition to providing the protein structure/conformation of AChE that appears to better accommodate arisugacin-like structures, the reported TB–*h*AChE[4b] bound structure provided conformational parameters (bond angles) for the presentation of the arisugacin ligands. It is apparent from our modeling efforts that AutoDock predicted binding affinities are very sensitive to ligand conformation, and further that modeling on its own does not arrive at what appears to be the ideal conformation (ideal meaning that specific conformation always exhibited the highest binding affinity regardless of the other variables introduced). With the conformation derived from the TB–*h*AChE structure (ideal conformation in this study), we examined the binding

affinity of the (+)-arisugacin A-DE-*anti* conformer [**Figure 2**] to the *tc*AChE model developed in our 2011 study (binding affinity of -16.4 kcal mol$^{-1}$ to *h*AChE, superior to that of the (+)-arisugacin A-DE-*syn* conformer with a binding affinity of -15.7 kcal mol$^{-1}$).

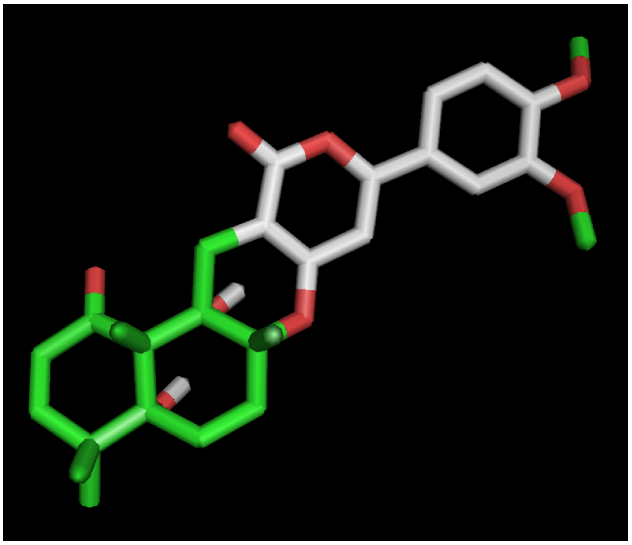

**Figure 2.** (+)-Arisugacin A-DE-*anti* TB–*h*AChE X-ray Based Conformation.

Note throughout our analyses the docking modes examined are those with the arisugacin scaffold docked such that the enone is proximal to the catalytic active site and the E-ring is in the peripheral anionic site (PAS) of the active site gorge. (+)-Arisugacin A-DE-*anti* conformer docked in this way in our 2011 *tc*AChE model (flexibility permitted in residues PHE330, TRP279, and ASP72) had a binding affinity of -9.6 kcal mol$^{-1}$. Docking this conformer in the *h*AChE model with flexibility permitted in residues TYR337, TRP286, and ASP74 (respective *h*AChE residues) we obtained a binding affinity of -14.2 kcal mol$^{-1}$. An overlay of the docking events into *h*AChE with the residues either flexible or locked reveals that the majority of conformational change occurs in the orientation of the residues [**Figure 3**, not the location of the conformationally locked ligand)] Why AutoDock modeling would arrive at a new higher energy well (geometry) than the original input conformation is not clear to us. However, we can see from this study that the TB–*h*AChE derived protein and conformation, rather than that derived from donepizil-*tc*AChE X-ray crystal structure appears to better accommodate the (+)-arisugacin A-DE-*anti* conformer in the binding mode of interest (-14.2 kcal mol$^{-1}$ versus -9.6 kcal mol$^{-1}$, flexibility permitted in respective residues).

Recall from our 2011 study[5], the docking mode we reported was the (+)-arisugacin A-DE-***syn*** conformer (-10.4 kcal mol$^{-1}$ binding affinity). During these docking studies we locked the conformations of the methoxy aryl groups to match the conformation of those of donepizil in the donepizil-*tc*AChE crystal structure, with the DE ring biaryl bond, as well as the two angular hydroxyl group bonds permitted to rotate. Interestingly, in this system the binding affinity of the (+)-arisugacin A-DE-*anti* conformer was predicted to be -8.2 kcal mol$^{-1}$. That is, the preference for the *anti* over the *syn* conformation is reversed. When we utilize the same ligand parameters (donepizil conformations of OMe's, with biaryl and hydroxyls with rotatable bonds) in docking experiments into the TB–*h*AChE derived protein conformation we found that the binding affinity for the (+)-arisugacin A-DE-*syn* conformer was -14.6 kcal mol$^{-1}$, and the (+)-arisugacin A-DE-*anti* conformer was not identified (100 geometries stored in a kcal mol$^{-1}$ range of -14.6 to -6.9). Reasoning that the inability to find the *anti* conformation docking event may result from a poor steric interaction between the locked MeO groups and the PAS residues, we performed the docking experiment with the same ligand parameters with flexibility introduced in residues TYR337, TRP286, and ASP74. Here the modeling predicted a binding affinity of the (+)-arisugacin A-DE-*anti* conformer of -12.5 kcal mol$^{-1}$ and the (+)-arisugacin A-DE-*syn* conformer was not found (100 geometries stored in a kcal mol$^{-1}$ range of -12.5 to -4.8). When we performed the docking experiment permitting bond rotation in residues TYR337, TRP286, and ASP74 and all the rotatable ligand bonds (aryl MeO bonds, DE ring biaryl bond, and two angular hydroxyl bonds) the binding affinity identified for the (+)-arisugacin A-DE-*syn* conformer was -11.5 kcal mol$^{-1}$, and the (+)-arisugacin A-DE-*anti* conformer was -11.2 kcal mol$^{-1}$. In the *tc*AChE model, the docking experiment with rotating bonds permitted in the respective residues and all the rotatable ligand bonds identified a binding affinity for the (+)-arisugacin A-DE-*syn* conformer of -9.7 kcal mol$^{-1}$, and for the (+)-arisugacin A-DE-*anti* conformer of -7.6 kcal mol$^{-1}$. With greater computational power/time perhaps these variations would be more tractable, nonetheless we feel it important these findings be presented.

**Figure 3.** Overlay of Docking with Residues TYR337, TRP286, and ASP74 Locked (Yellow) or Flexible (Magenta)

**Docking Experiments with Varying Degrees of Freedom**.

As noted, generally both ligand and protein conformations oriented and locked to match those observed in the TB–*h*AChE X-ray crystal structure had the higher affinity predictions. To our surprise, visual examination of binding events with differing degrees of permitted freedom revealed seemingly small/subtle variations in geometry that are accompanied by large binding affinity differences. Herein are illustrative examples.

**Figure 4.** Overlay of Docking with Aryl-OMe Bonds Locked (Magenta) or Rotatable (Green).

When docking the (+)-arisugacin A-DE-*anti* conformer (geometry based on geometry of TB in TB–*h*AChE X-ray crystal structure) into the TB–*h*AChE derived protein structure (no flexible residues) with the methoxy-aryl groups either locked or free to rotate, binding events of seemingly very similar geometries were identified with a binding affinity difference of 1.7 kcal $mol^{-1}$ (binding affinity of the locked ligand was -16.4 kcal $mol^{-1}$, that of the ligand with rotatable MeO's was -14.7 kcal $mol^{-1}$). An overlay of these binding events revealed that the main difference resides in a small change in the bond angle of the aryl-methoxy bonds [**Figure 4**, not the location of the ligands].

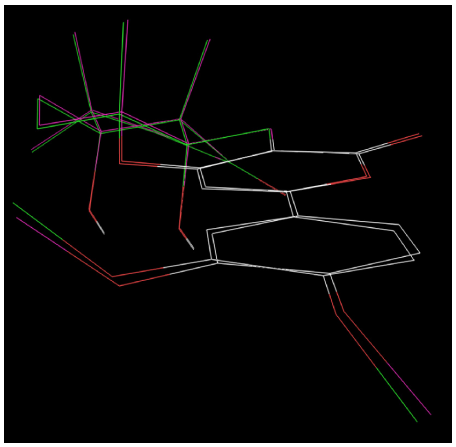

**Figure 5.** Overlay of Docking with DE Ring Biaryl Bond Locked (Magenta) or Rotatable (Green).

When docking the (+)-arisugacin A-DE-*anti* conformer (geometry based on geometry of TB in TB–*h*AChE X-ray crystal structure) into the TB–*h*AChE derived protein structure (no flexible residues) with the DE ring biaryl bond either locked or free to rotate, binding events of seemingly very similar geometries are identified with a binding affinity difference of 0.9 kcal $mol^{-1}$ (binding affinity of the locked ligand was -16.4 kcal $mol^{-1}$, that of the ligand with a rotatable biaryl bond was -15.5 kcal $mol^{-1}$). An overlay of these binding events revealed that the main difference appears to be a small change in the biaryl bond angle [**Figure 5**, not the location of the ligands].

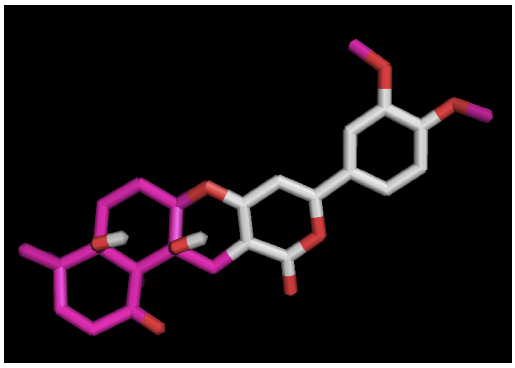

**Figure 6.** (+)-Arisugacin A-DE-*anti* Angular Hydroxyl Group Hydrogen Atom Positioning.

When it came to positioning the hydrogen atoms of the angular hydroxyl groups, we had to relay on our intuition [**Figure 6**]. We chose to place the 12a-OH-hydrogen such that it could engage the pyran oxygen in a H-bonding interaction (similar to H-bonding of gauche vicinal diols). The hydrogen atom of the 4a-OH-Hydrogen was position such that it could H-bond to the 12a-OH, and the geometry was optimized using molecular mechanics (MM2 in CS Chem3D Ultra®).

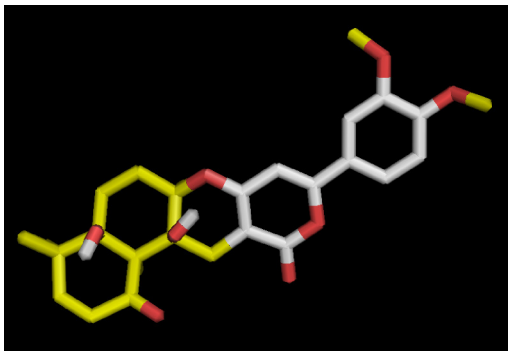

**Figure 7.** Docking Event with Angular Hydroxyl Group Bonds Permitted to Rotate.

Docking the (+)-arisugacin A-DE-*anti* conformer with the two angular hydroxyl group bonds free to rotate provided a binding event with differing hydrogen atom positioning [**Figure 7**]. The binding affinity difference was -0.9 kcal $mol^{-1}$ (binding affinity of the locked ligand was -16.4 kcal $mol^{-1}$, that of the ligand with rotatable angular hydroxyl group bonds was -15.5 kcal $mol^{-1}$).

## References and notes


1. For references on AutoDock, see: **Version 4.2** (a) Morris, G.; Goodsell, D.; Halliday, R.; Huey, R.; Hart, W.; Belew, R.; Olson, A. J. *J. Comp. Chem.* **1998**, *19*, 1639. **Vina** (b) Trott, O.; Olson, A. J. *J. Comp. Chem.* **2010**, *31*, 455.
2. The PyMOL Molecular Graphics System (2002), available at http://www.pymol.org.
3. Python Molecule View: Sanner, M. F. *J. Mol. Graphics Modell.* **1999**, *17*, 57.
4. For X-ray crystal structure data, see: **Donepezil** (a) Kryger, G.; Silman, I.; Sussman, J. L. *Structure Fold. Des.* **1999**, *7*, 297. **Territrem B** (b) Cheung, J.; Gary, E. N.; Shiomi, K.; Rosenberry, T. L. *ACS Med. Chem. Lett.* **2013**, *4*, 1091.
5. Al-Rashid, Z. F.; Hsung, R. P. *Bioorg. Med. Chem. Lett.* **2011**, *21*, 2687.
6. Davis, I. W.; Leaver-Fay, A.; Chen, V. B.; Block, J. N.; Kapral, G. J.; Wang, X.; Murray, L. W.; Bryan Arendall, B. III; Snoeyink, J.; Richardson, J. S.; Richardson, D. C. *Nucleic Acids Res.* 2007, *35*, 375. Web-based algorithm made available through molprobity.biochem.duke.edu.